LA-UR-17-29832
Approved for public release; distribution is unlimited.

Title: Foil focusing of relativistic electron beams

Author(s): Ekdahl, Carl August Jr.

Intended for: Report

Issued: 2017-10-26

Foil Focusing of Relativistic Electron Beams

Carl Ekdahl

***Abstract*—When an intense relativistic electron beams (IREB) passes through a grounded metal foil, the transverse electric field due to the beam space charge is locally shorted out, and the beam is focused by the magnetic field of its current. The effect can be treated as focusing by a thin lens with first order aberration. Expressions for the focal length and aberration coefficient of the equivalent thin lens are developed in this note. These are then applied to practical examples representative of IREB research at Los Alamos National Laboratory.**

***Index Terms*—Intense relativistic electron beams, space charge, linear induction accelerators**

I. Introduction

THE use of a thin conducting foil placed orthogonal to a high-current electron beam in order to short out the transverse space-charge electric field is a well-known technique for focusing the beam [1]. The same effect can be obtained with less increase in beam emittance by using a highly-transparent grid of fine wires [2]. Arrays of foils or grids have been used to stably transport intense relativistic electron beams (IREBs) for significant distances [3, 4, 5, 6], transport through accelerators [7], and have even been proposed as an effective means of focusing electron beams for flash radiography [8] .

In this article, a method for simply calculating the focal length of a foil or grid is developed. For many practical applications, this reduces to a simple formula for estimation of the focal length. This is useful for experiments on the DARHT accelerators, where beam intercepting foils are frequently used for beam imaging [9, 10, 11] and generation of warm dense matter [12].

Foils or grids can also cause the beam to filament, because they short out the space-charge fields that balance the tendency of the current to pinch [13]. Estimates of the filamentation growth rate for DARHT parameters are beyond the scope of this note, and are relegated to future work.

In what follows, in Section II we develop a simple expression for foil focusing based on the thin-lens model. Section III is devoted to a few practical examples, and is followed by some conclusions in Section IV.

Thiss work was supported by the National Nuclear Security Administration of the U. S. Department of Energy under contract number DE-AC52-06NA25396.

Carl. Ekdahl is with the Los Alamos National Laboratory, Los Alamos, NM 87545 USA (e-mail: cekdahl@lanl.gov).

II. Theory

The deflection of a relativistic electron's trajectory when transiting a thin lens is $\delta r' = \delta p_r / p_z$, where δp_r is the "kick" in transverse momentum $p_r 0$, and $p_z >> p_r$ is the longitudinal momentum. This kick is provided by the foil shorting out the transverse electric field. Foils are usually placed normal to the beam for focusing, or production of warm dense matter. They are usually placed at an angle for accurate imaging. Transparent grids of fine wires can also be used for focusing if the openings are less than about a Debye length [5, 7].

A. Foil Normal to Beam

Adler solved for this deflection by a conducting foil normal to the beam direction. In this geometry, the magnetic boundary conditions are satisfied without needing an image current, so the one need only use an image charge to satisfy the boundary conditions at the foil by cancelling the net transverse electric field there. Adler's result is

$$\frac{\delta p_r}{p_z} = -16\frac{I_b}{I_A}\left(\frac{b}{a}\right)\sum_{n=1}^{\infty}\frac{J_1\left(\chi_{0n}a/b\right)J_1\left(\chi_{0n}r/b\right)}{\chi_{0n}^3 J_1\left(\chi_{0n}\right)^2} \tag{1}$$

where a is the beam radius, b is the beam-tube radius, I_b is the beam current, and $I_A = 17.05\beta\gamma$ kA is the Alfven limiting current. Also, χ_{0n} is the nth zero of the zero order Bessel function $J_0(z)$. The sign indicates focusing by the un-neutralized beam current.

In practice, the beam size is usually less than one-half the tube size at the foil, $b/a \geq 2$. Eq. (1) is plotted in Figure 1 as a function of particle position r/a for a few different values of b/a . From this plot it is clear that the strongest focusing by a foil is for the smallest beams (largest b/a). Also note that the edge effects are defocusing, rather than focusing as for a spherical aberration.

Obviously, from the power series expansion of $J_1(z)$ and inspection of Figure 1, for small values of r/a Eq. (1) collapses to r/a times a function of b/a . Thus, the full curve can be approximated by a thin lens with a first order aberration to account for the edge defocusing.

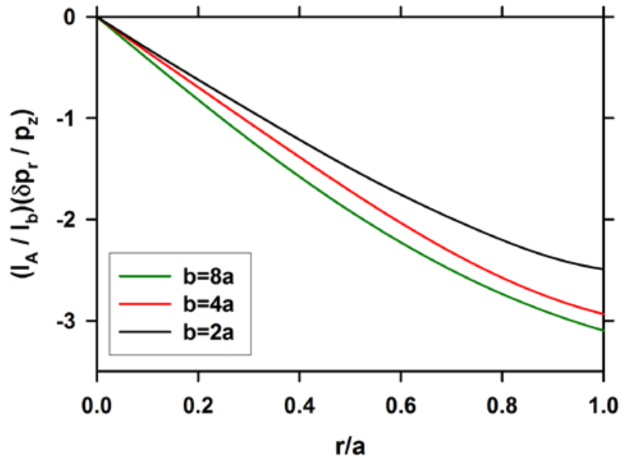

Figure 1: Deflection of electrons due to foil focusing as a function of distance from beam center, *r*. Beam envelope radius is *a* and beam pipe radius is *b*. Deflection for three different values of *b/a* is shown.

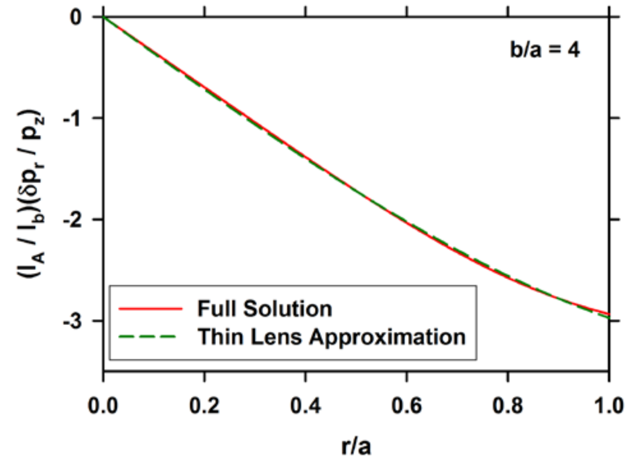

Figure 2: Deflection calculated from the full solution, Eq. (1), shown as red curve, compared with that calculated from the thin lens approximation, Eq. (3), shown as green dashed curve. The scaled focal length used was $f_a = 0.278150$ and the scaled aberration coefficient was $C_a = -0.173177$.

The beam optics equation for deflection by a thin lens with a first order spherical aberration is

$$\delta r' = -\frac{r}{f}\left[1 + C_1 r^2\right] \tag{2}$$

where f is the focal length, and C_1 is the coefficient of aberration. For foil focusing, both the coefficient of aberration and the focal length are functions of b/a. Note that the aberration in foil focusing causes edge defocusing. This is just the opposite of the effect of spherical aberration of a solenoid, which causes edge focusing. Eq. (2) can be related to Eq. (1) with r/a as the variable by using the substitutions $f_a = \left(I_b / I_A\right) f / a$ and $C_a = C_1 a^2$;

$$\delta r' = -\frac{I_b}{I_A}\frac{r/a}{f_a}\left[1 + C_a \left(r/a\right)^2\right] \tag{3}$$

The scaled focal length f_a and scaled aberration coefficient C_a can now be found by least squares fitting Eq. (3) to the solution given by Eq. (1). For example, for $b = 4a$, Figure 2 compares the full solution of Eq. (1) with Eq. (2) using parameters arrived at by least square fitting. Here, it is seen that the thin lens approximation is adequate for most experimental applications.

TABLE I
SCALED PARAMETERS FOR THIN LENS APPROXIMATION

b/a	$f_a = \left(I_b / I_A\right) f / a$	$C_a = C_1 a^2$
1.5	0.352670	-0.229686
2	0.318043	-0.199032
4	0.278150	-0.173177
8	0.262449	-0.160402
16	0.255143	-0.155948

The least square fit parameters for other values of b/a that might arise in experiments are shown in Table I. Intermediate values can be found by interpolation. Moreover, the scaled focal length converges to ~0.24 and the aberration coefficient to ~0.16 for b/a greater than 16. Most experiments at DARHT have $b/a \geq 4$, so a useful approximation is $f = (I_A / 4I_b)\, a$, which is no more than ~10% inaccurate.

B. Foil Angled to Beam

Angling the foil to the beam direction for the purpose of beam imaging creates a transverse steering force in addition to the focusing force discussed thus far. In this case one needs an image current as well as the image charge in order to satisfy the boundary conditions on the conducting foil. Therefore, the resulting steering force is order $1/\gamma^2$ of the focusing force, and can be neglected for highly relativistic beams.

III. APPLICATION

Some examples of the application of the thin-lens approximation to DARHT-like experiments are discussed in this section.

A. DARHT-I

Beam imaging is frequently performed within a meter of the DARHT-I injector. The 1.7 kA beam energy at this position is ~3.8 Mev, so $I_b / I_A = 1.194 \times 10^{-2}$. During imaging for an emittance measurement using the focal scan technique, the beam size at the foil ranges from mm to ~2 cm maximum. In the 6-inch beam pipe, this gives b/a over a range from ~3.75 to > 50. For the largest beams, the focal length is $f \approx 46$ cm and for the smallest beam o target $f \approx 20a$. Thus, for a beam focused to 2-mm FWHM, the focal spot from foil focusing would be < 2 cm downstream of the target (in the absence of other beam target effects).

After the accelerator exit, the beam has been accelerated to ~ 20 MeV, and $I_b / I_A = 2.55\times10^{-3}$. Therefore, the foil focal length is very long for the largest beam size, but the smallest focused beams still have short focal lengths. Again using the 2-mm FWHM beam example, the focal point would be < 9.4 cm downstream of the foil.

B. DARHT-II

All beam imaging on DARHT-II has been done after the LIA exit, so the 1.7-kA, 16.5-MeV beam gives $I_b / I_A \approx 3\times10^{-3}$. The foil focusing focal length for large beams is $f \approx 94a$ and for small beams it is $f \approx 80a$.

C. Scorpius

Scorpius will have a lower energy injector than DARHT-I, producing a ~2-kA, ~2-MeV beam, giving $I_b / I_A \approx 2.4\times10^{-2}$. Therefore, imaging foils between the injector and LIA would have a focal length of $f \approx 11a$.

IV. Conclusion

A thin lens approximation to the focusing effect of conducting foils. The focal length is proportional to the beam size, and inversely proportional to I_b / I_A . Thus, for DARHT-class electron beams with $I_b / I_A << 1$, the focal length can be quite long for a large beam. However, the focal length can be very short if the beam is focused onto a foil during the course of an emittance measurement.

A direct measurement of the foil focusing effect for DARHT-class beams would make for an interesting experiment that would provide confidence in the theory. A two-foil geometry similar to that used in [14] would enable such a measurement.

Appendix

The sum in Eq. (1) converges rather slowly, so a large number of terms are needed for accuracy. For this note, 100 terms were used. The required Bessel zeros χ_{0n} were taken from a table for $n \le 20$. Larger zeros were approximated with

$$\chi_{0n} = (n - 1/4)\pi \qquad (4)$$

which is derived from the asymptotic form for $|z| \to \infty$

$$J_1(z) = \sqrt{2/(\pi z)}\cos(z - 3\pi/4) \qquad (5)$$

Acknowledgment

As always, the author thanks his colleagues at Los Alamos and elsewhere for stimulating discussions and enlightenment.

References

[1] R. J. Adler, "Image-field focusing of intense ultra-relativistic electron beams in vacuum," *Part. Accel.*, vol. 12, pp. 39 - 44, 1982.

[2] S. Humphries and C. Ekdahl, "Image charge focusing of relativistic electron beams," *J. Appl. Phys.*, vol. 63, no. 2, pp. 583 - 585, 1988.

[3] R. J. Adler, B. Sabol and G. F. Kiuttu, "Alternate transport techniques for electron induction linacs," *IEEE Trans. Nucl. Sci.*, vol. 30, no. 4, pp. 3198 - 3200, 1983.

[4] S. Humphries, "Equilibria for foil-focused relativistic electron beams," *Part. Accel.*, vol. 13, pp. 249 - 253, 1983.

[5] S. Humphries and C. Ekdahl, "Experiments on intense electron beam transport in mesh focusing arrays," in *Part. Accel. Conf.*, 1989.

[6] J. A. Antoniades and et al., "High-current beam transport using foil focussing," in *Pulsed Power Conf.*, 1989.

[7] C. Ekdahl and et al., "HITMI: Experiments with an electron-beam driven vacuum linear induction accelerator," in *Int Conf. High Power Part. Beams*, 1992.

[8] C. Ekdahl and S. Humphries, "Grid-focused diodes for radiography," in *Pulsed Power Conf.*, Monterey, CA, USA, 2005.

[9] C. Ekdahl and e. al., "First beam at DARHT-II," in *Part. Accel. Conf.*, 2003.

[10] C. Ekdahl, E. O. Abeyta, H. Bender, W. Broste, C. Carlson, L. Caudill, K. C. D. Chan, Y.-J. Chen, D. Dalmas, G. Durtschi, S. Eversole, S. Eylon, W. Fawley, D. Frayer, R. Gallegos, J. Harrison, E. Henestroza, M. Holzscheiter, T. Houck, T. Hughes, S. Humphries, D. Johnson, J. Johnson, K. Jones, E. Jacquez, B. T. McCuistian, A. Meidinger, N. Montoya, C. Mostrom, K. Moy, K. Nielsen, D. Oro, L. Rodriguez, P. Rodriguez, M. Sanchez, M. Schauer, D. Simmons, H. V. Smith, J. Studebaker, R. Sturgess, G. Sullivan, C. Swinney, R. Temple, C. Y. Tom and S. S. Yu, "Initial electron-beam results from the DARHT-II linear induction accelerator," *IEEE Trans. Plasma Sci.*, vol. 33, no. 2, pp. 892 - 900, 2005.

[11] J. E. Coleman, D. C. Moir, C. A. Ekdahl, J. B. Johnson, B. T. McCuistian, G. W. Sullivan and M. T. Crawford, "Increasing the intensity of an induction accelerator and reduction of the beam breakup instability," *Phys. Rev. STAB*, vol. 17, no. 3, p. 030101, 2014.

[12] J. E. Coleman and J. Colgan, "Spatially and temporally resolved measurements of a dense copper plasma heated by intense relativistic electrons.," *Phys. Plasmas*, vol. 24, p. 083302, 2017.

[13] S. Humphries and C. Ekdahl, "Filamentation instability of a relativistic electron beam in a foil transport channel," *Part. Accel.*, vol. 24, pp. 147 - 162, 1989.

[14] C. Vermare, H. A. Davis, D. C. Moir and T. P. Hughes, "Ion emission from solid surfaces induced by intense electron beam impact," *Phys. Plasmas*, vol. 10, no. 1, pp. 277 - 284, Jan. 2003.